

Activation of Au/TiO₂ Catalyst for CO Oxidation

Jeff H. Yang,[†] Juan D. Henao,[†] Mpfunzeni C. Raphulu,[‡] Yingmin Wang,[§] Tiziana Caputo,^{||} A. J. Groszek,[⊥] Mayfair C. Kung,[†] Michael S. Scurrell,[‡] Jeffrey T. Miller,[○] and Harold H. Kung^{*,†}

Department of Chemical and Biological Engineering and Department of Materials Science and Engineering, Northwestern University, Evanston, Illinois, 60208-3120, Molecular Sciences Institute, School of Chemistry, University of Witwatersrand, Johannesburg, South Africa, Microscal Ltd., London, United Kingdom W10 5AL, and BP Research Center, E-1F, Naperville, Illinois 60563

Received: February 16, 2005; In Final Form: March 29, 2005

Changes in a Au/TiO₂ catalyst during the activation process from an as-prepared state, consisting of supported AuO_x(OH)_{4-2x}⁻ species, were monitored with X-ray absorption spectroscopy and FTIR spectroscopy, complemented with XPS, microcalorimetry, and TEM characterization. When the catalyst was activated with H₂ pulses at 298 K, there was an induction period when little changes were detected. This was followed by a period of increasing rate of reduction of Au³⁺ to Au⁰, before the reduction rate decreased until the sample was fully reduced. A similar trend in the activation process was observed if CO pulses at 273 K or a steady flow of CO at about 240 K was used to activate the sample. With both activation procedures, the CO oxidation activity of the catalyst at 195 K increased with the degree of reduction up to 70% reduction, and decreased slightly beyond 80% reduction. The results were consistent with metallic Au being necessary for catalytic activity.

Introduction

Although bulk gold has historically been regarded as chemically inert, highly active catalysts of gold on metal oxides have been reported in recent years for various reactions,¹⁻³ including remarkable activity for low-temperature CO oxidation. In particular, Au/TiO₂ exhibits CO oxidation activity at temperatures as low as 90 K.⁴ The intense effort expanded on the elucidation of the origin of the high activity and factors that influence it⁵⁻¹⁰ has led to different models of the Au active site. However, as yet there are no overarching conclusions to account for all the observations. Metallic Au has been proposed to be the active site, with some proponents advocating that the highest activity occurred when two layers of Au atoms are deposited on a TiO₂ surface.^{11,12} Others report that Au cations in the absence of metallic Au atoms also exhibit catalytic activity.^{13,14} Another model portrays the active site as an ensemble of metallic Au clusters with Au cations at the perimeters of such clusters.^{3,15} Although there is yet no direct evidence in support of this latter model, it was shown that metallic Au alone is insufficient for high catalytic activity.^{16,17}

The most common method to prepare a highly active Au/TiO₂ catalyst is by deposition–precipitation, in which most likely a [AuO_x(OH)_{4-2x}]ⁿ⁻ species is deposited on the support.¹⁸ In the earlier studies, the sample would be activated by calcination in air at 200–400 °C. More recent reports indicated that more active catalysts can be obtained by activation in other

gases and/or at lower temperatures.^{19,20} For example, Schumacher et al. reported that H₂ treatment at 200 °C yielded catalysts that were significantly more active than the calcined ones.²⁰ We observed that H₂ reduction at 298 K is also an effective activation method. The CO oxidation activity of a catalyst activated with this procedure was 0.29 mol of CO (mol Au·min)⁻¹ at 195 K in a feed of 1% CO, 2.5% O₂, and balance He. This rate was more than 3 times higher than that of the calcined Au/TiO₂ catalyst distributed by the World Gold Council (Lot No. 02-4, 1.5 wt %, 3.8 nm Au particle diameter) under the same conditions, which was 0.08 mol CO (mol Au·min)⁻¹. Since it is possible to reduce a catalyst with H₂ pulses at room temperature, thereby controlling the degree of reduction, we may be able to monitor the relationship among the average Au oxidation state, Au metal cluster size, and catalytic activity during the activation process. Alternatively, we could also perform reduction with CO at subambient temperatures for comparison. Here we report the investigation using these two activation methods.

Experimental Section

Catalyst Preparation. The Au/TiO₂ catalyst was prepared by deposition–precipitation with HAuCl₄ (Aldrich, 99.999%) as the precursor and microrutile as the support (Sachtleben, approximately 200 m² g⁻¹). The HAuCl₄ solution (0.014 M) was neutralized slowly with vigorous stirring to pH 7 at 70 °C with a NaOH solution and mixed with a TiO₂ suspension that was kept at 35 °C. The resulting mixture was maintained at pH 7 at 35 °C for an hour. The mixture was filtered, and the solid was washed twice with room temperature deionized water and then once with 70 °C water. The solid was suction filtered and dried at room temperature. The resulting sample is referred to as the as-prepared sample. The Au content was determined by X-ray fluorescence (XRF) to be 7.0 wt %. This sample was used for all experiments except the CO pulse reduction at 273 K. A 4 wt % sample prepared similarly was used there.

* Address correspondence to this author. E-mail: hkung@northwestern.edu.

[†] Department of Chemical and Biological Engineering, Northwestern University.

[‡] University of Witwatersrand.

[§] Department of Materials Science and Engineering, Northwestern University.

^{||} On leave from Department of Chemical Engineering, University of Naples “Federico II”, Italy.

[⊥] Microscal Ltd.

[○] BP Research Center.

H₂ and CO Pulse Reduction. In a typical experiment for H₂ reduction, 0.1 g of as-prepared Au/TiO₂ sample was placed in a fused silica, U-tube microreactor, supported between two layers of acid-washed quartz wool. The reactor was purged with Ar (Matheson, 99.999%) at a flow rate of 50 cm³ min⁻¹. Any O₂ impurity in the Ar stream was removed with a MnO trap located immediately downstream of the mass flow controller. Hydrogen reduction was accomplished by injecting 0.5 cm³ pulses of pure H₂ (Matheson, 99.999%) into the Ar stream. A molecular sieve trap was located downstream of the reactor to remove any water that might be produced during reduction. The consumption of H₂ was determined with a TCD detector in a HP 5890 gas chromatograph. For pulse reduction during X-ray absorption measurements, a pulse system similar to the one above was used together with a flow-through sample cell for XAS and a N₂ flow of 100 cm³ min⁻¹. The pulse size was ca. 0.6 cm³ pure H₂.

CO pulse reduction at 273 K was conducted also in a U-tube microreactor, using 0.012 g of a 4 wt % Au/TiO₂. After purging the reactor with 100 cm³ min⁻¹ of high purity He that was further purified with a reduced MnO₂ trap to remove O₂, 0.5 cm³ pulses of 10% CO in He were passed over the catalyst, and the consumption of CO was monitored by a TCD detector.

Catalytic Activity for CO Oxidation. When desired, CO oxidation at 195 K was also conducted during H₂ pulse reduction in the U-tube microreactor. After reducing a catalyst by a certain number of pulses, the catalyst was first cooled to 195 K using an acetone–dry ice bath while in an Ar gas flow. Then, the gas was switched to the reactant gas flow (1% CO, 2.5% O₂ and balance He, 50 cm³ min⁻¹) by a switching valve. The CO concentration in the effluent was continuously monitored by IR spectroscopy with a gas cell. After CO oxidation, the catalyst bed was purged with Ar for approximately 15 min at 195 K to remove CO and O₂ before warming up to room temperature for subsequent H₂ pulse reduction. This step is critical because we have shown previously that as-prepared Au/TiO₂ catalyst can be rapidly reduced by the reaction mixture at room temperature.²¹

X-ray Absorption Spectroscopy (XAS). XAS experiments were carried out at the bending magnet Beamline 5-BMD of the Dupont-Northwestern-Dow Collaborative Access team at the Advanced Photon Source at Argonne National Laboratory in Argonne, IL.¹⁹ Higher harmonics in the X-ray beam was minimized by detuning the Si(111) monochromator by about 15% at the Au L_{III} edge (11.919 keV). The spectra were collected in the transmission mode with use of a flow-through sample cell with Kapton windows. The cell consisted of two concentric cylinders with the inner cylinder only about half the length of the outer cylinder. Gas entered via the outer cylinder, swept through the region between the two cylinders, then passed through the inner cylinder before exiting the sample cell. Because of rather extensive backmixing of the gases, it took about 3 min for a complete (>99.5%) sweep of the gas in the cell. About 0.15 g of sample was used to make a self-supporting pellet that was sandwiched between two nylon grids and placed at the end of the inner cylinder, near the center of the sample cell. All XAS data were collected during N₂ purge at room temperature and the XAS measurement typically took 10–25 min depending on the type of scan. We have determined that the XAS measurements did not cause any detectable change in a sample, if the sample had not been previously reduced or reduced only slightly (<5%), i.e., consecutive scans showed no detectable differences. However, if the sample had been previously reduced by 5% or more, then the X-ray beam induced

further reduction of the sample, as evidenced by a decrease in the near edge intensity in the consecutive XANES spectrum.

Both the XANES and EXAFS data were analyzed by using standard procedures with the WINXAS97 software. Phase shifts, backscattering amplitudes, and XANES references were obtained from reference compounds: Au₂O₃ for Au³⁺–O, and Au foil for Au⁰ and Au–Au. The XANES fits of the normalized spectra were made by a linear combination of experimental standards. The EXAFS coordination parameters were obtained by a least-squares fit in the *k*- and *r*-space of the isolated multiple-shell, *k*²-weighted Fourier transform data.

Transmission Electron Microscopy (TEM) and XPS. TEM examination of Au/TiO₂ samples was performed with a Hitachi HF-2000 TEM with a field emission gun at 200 keV. XPS of the catalysts was conducted in a Perkin-Elmer/PHI XPS system with Al K α radiation (1486.6 eV), using a dual-anode X-ray source with spherical electron energy analyzer. The powder samples were mounted onto the sample holders with carbon tape. They were then placed in the outer chamber of the spectrometer and pumped to vacuum overnight. The spectra were collected with an anode voltage of 15 kV and an emission current of 20 mA. Different energy regions were scanned to obtain separate spectra for carbon, oxygen, titanium, and gold. The 1s binding energy for carbon, 284.7 eV, was used to correct for the shift in energy for all components due to electrostatic charging of the samples.

Microcalorimetry. Calorimetric measurements were performed with 0.1 g of catalyst in a Microscal flow microcalorimeter. At room temperature, 0.66 cm³ of pure H₂ in a N₂ carrier gas flow of 1 cm³ min⁻¹ was pulsed through the catalyst and the H₂ consumption and heat evolved after each pulse were measured.

In Situ Infrared Spectroscopy. Infrared spectroscopy (IR) was conducted in a stainless steel IR cell fitted with CaF₂ windows at subambient temperatures in a Nicolet Nexus 670 FTIR spectrometer. To achieve the desired temperature, the IR cell was brought into contact with a copper housing containing a liquid nitrogen and dry ice mixture. A self-supporting pellet was made by pressing 10 mg of as-prepared sample mixed with an equal amount of anatase. A thermocouple, placed near the pellet, records the temperature of the gas immediately after passing through the pellet. The volume of the IR cell was about 6 cm³. Thus, the gas in the cell could be changed reasonably rapidly with a gas flow of 11 cm³ min⁻¹. Reaction with this cell was conducted with 1% CO, 2.5% O₂, and the balance He. The effluent gas of the IR cell was analyzed with a HP 6890 gas chromatograph. The spectra presented are referenced to the sample in He at the same temperature, with contributions from gaseous CO removed.

Results

H₂ and CO Pulse Reduction. The amounts of H₂ consumed in each pulse in a microreactor experiment are plotted in Figure 1 as a function of the pulse sequence. Within uncertainties (± 0.1 μ mol H₂), there was no consumption of H₂ in the first 10 pulses. Following this initial induction period, the consumption of H₂ slowly increased in the next 5 pulses, and accelerated after that, reaching a maximum at pulse 26. H₂ consumption in subsequent pulses decreased gradually, and approached a steady-state value equivalent to about 0.2 μ mol of H₂ after pulse 50. The total amount of Au³⁺ that was reduced by the H₂ pulses in the experiment was determined from the area under the curve up to pulse 58 in Figure 1, and found to be 6.8 Au wt %, which was in good agreement with the 7.0 Au wt % determined by XRF.

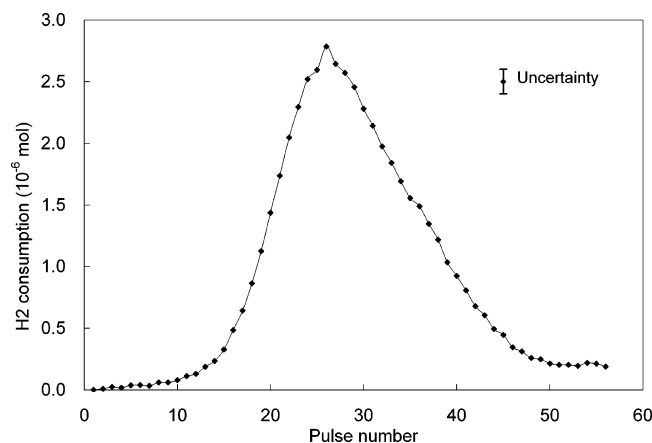


Figure 1. H₂ consumption at 298 K as a function of pulse sequence; 100 mg of a 7 wt % Au/TiO₂ catalyst.

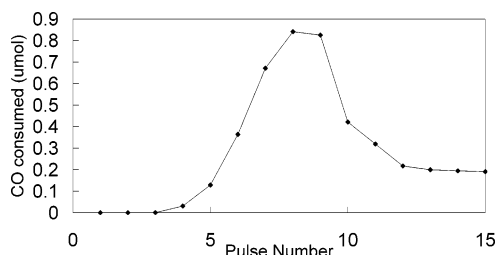


Figure 2. CO consumption at 273 K as a function of pulse sequence, 12 mg of a 4 wt % Au/TiO₂ catalyst.

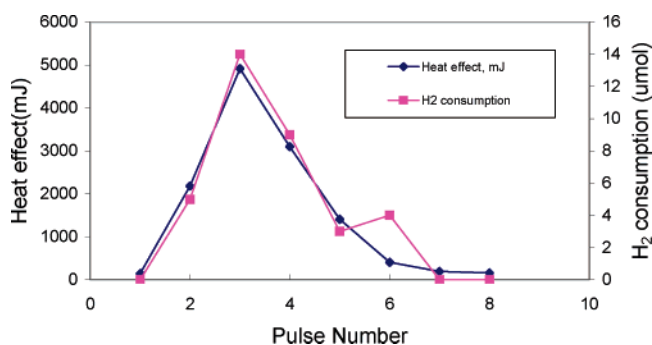


Figure 3. H₂ consumption and heat evolved in calorimetry experiment as a function of pulse sequence

Figure 2 shows the CO consumption per pulse at 273 K as a function of the pulse sequence. The CO consumption showed a similar trend as for H₂ consumption. There was little uptake in the first few pulses before significant consumption commenced.

Microcalorimetry. The H₂ consumption in the calorimetry experiment followed a similar trend when H₂ pulses were passed through the catalyst, as shown in Figure 3. The first H₂ pulse did not yield measurable H₂ consumption while the second pulse showed a significant increase in H₂ consumption, which eventually reached a maximum at the third pulse. The heat evolved from the reduction of the catalyst had an almost identical trend as the H₂ consumption. The integral heat per mole of H₂ consumed was calculated to be 400 ± 62 kJ/mol. This high value was consistent with reduction of Au³⁺ instead of adsorption of H₂. For reference, the heat of formation of water at room temperature is -285.8 kJ/mol.

XPS. The oxidation state of Au on the surface of a sample that had been reduced by H₂ pulse to ca. 50% was determined with XPS. The sample was removed from the microreactor after 26 H₂ pulses. Figure 4 shows the spectrum obtained, together

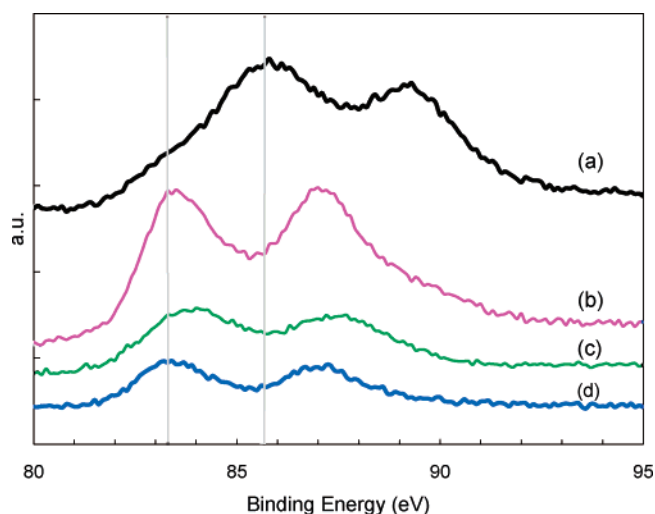


Figure 4. Au (4f) binding energy of Au/TiO₂ catalyst: (a) as-prepared sample; (b) sample fully reduced by H₂ pulses; (c) sample reduced by H₂ pulses to ca. 50%; and (d) reference Au/TiO₂ catalyst (calcined) distributed by WGC.

with those of an as-prepared and a completely reduced sample. In all samples, the characteristic doublets of Au 4f_{7/2} and 4f_{5/2} peaks were observed. The two peaks for the as-prepared catalyst were at 85.8 and 89.1 eV, which are similar to those reported on Au³⁺ compounds,⁹ while those of the fully reduced catalyst were at 83.2 and 87.0 eV. The latter agree very well with those of the reference Au/TiO₂ catalyst distributed by the World Gold Council (WGC). For the 50% reduced sample, the two peaks were broader, and the maxima appeared intermediate between the other two samples, which is in agreement with the expectation that a mixture of Au oxidation states was present. The oxidation state of the 50% reduced sample was independently determined by XAS measurement (data not shown). With use of a linear combination of Au³⁺ and Au⁰ XANES spectra, the percentage of Au³⁺ reduced was determined to be 55%.

XAS. The reduction of Au³⁺ species by H₂ pulses at 295 K was also monitored by XAS. Figure 5 shows the XAS spectra as a function of pulse sequence. The spectrum of the as-prepared sample showed an intense white line at the Au L_{III} edge, typical of supported Au³⁺ species.¹⁹ Within experimental uncertainties, the intensity of the white line remained unchanged for the first 5 pulses, and began to decrease afterward, indicating detectable reduction of Au³⁺ to Au⁰. By using a linear combination of XANES spectra of Au³⁺ and Au⁰ reference compounds, the percentage of Au³⁺ and Au⁰ in the sample was determined. The decrease in the percentage of Au³⁺ after each pulse is shown in Figure 6. The curve in Figure 6 showed a similar trend as Figure 1: an induction period followed by increasingly faster and then decreasing reduction rate.

EXAFS analysis was carried out on this set of spectra. Figure 7 shows the magnitude of the Fourier transformed, k^2 -weighted χ function of selected EXAFS spectra in R -space. The positions corresponding to Au–O and Au–Au scatterings are indicated by arrows. The magnitude of transform due to the Au–O scattering barely decreased from pulse 1 to pulse 5, and then much more rapidly, particularly between pulse 8 and 14. After pulse 15, there was little Au–O scattering. In contrast, there was little Au–Au scattering until pulse 9. The Au–Au scattering then increased, reaching a maximum value at pulse 16. At this point, assuming hemispherical particles, the coordination number (CN) of about 6 at pulse 16 corresponded to a particle of about 1.0 nm in diameter.²²

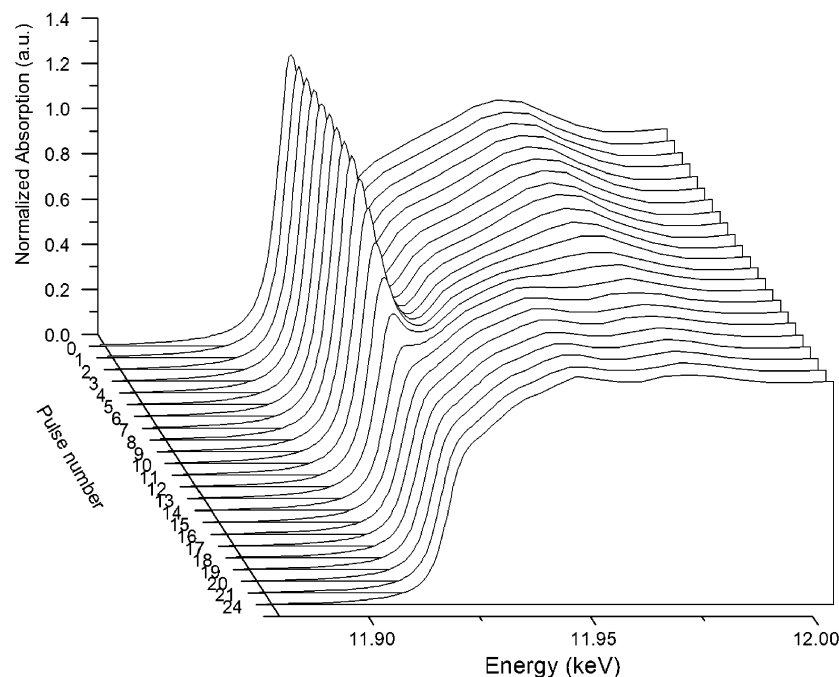


Figure 5. XANES spectra as a function of H_2 pulse sequence.

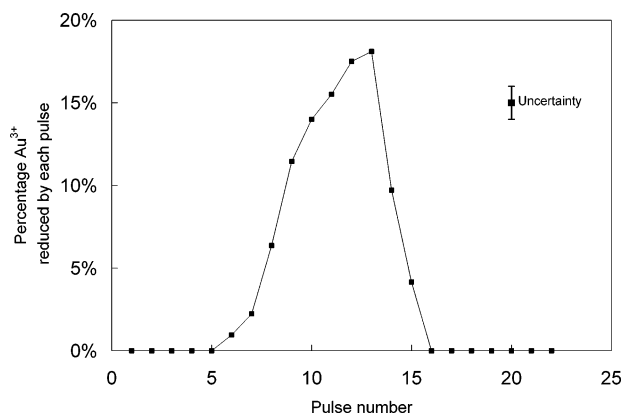


Figure 6. Percentage of Au^{3+} reduced by each H_2 pulse as a function of pulse sequence in the XAS experiment.

The change in the Au–Au coordination number with pulse sequence is plotted in Figure 8, along with the fractions of Au^{3+} and Au^0 as determined by XANES. Since the Au–Au coordination arises from metallic Au clusters only, it is necessary to correct the magnitude of the Fourier transform by the fraction of metallic Au in the sample in order to obtain the accurate value for the metal clusters. If we assume that Au^{3+} and Au^0 exist in separate phases, then the corrected Au–Au CN in the metallic portion of the sample can be estimated by dividing the CN by the fraction of metallic Au.²³ These corrected values are plotted also in Figure 8. Except for pulses 9 and 10, where the uncertainties were large because of the small amounts of Au^0 and low Fourier transform magnitudes, the corrected Au–Au CN was around 6 ± 0.5 , possibly increasing from 5.5 to 6 with increasing extent of reduction. This suggests that the Au particles rapidly attained an average size of about 1.0 nm once they are formed, and grew slowly to about 1.5 nm when the sample was fully reduced. XAS parameters of selected pulses are shown in Table 1. The Au–Au bond distance was 2.75 Å for particles with Au–Au CN of 6.0, which is shorter than the 2.88 Å for bulk Au. The shortening of Au–Au bond distance

with smaller CN has been reported recently by Schwartz et al. for Au on titania-based supports²⁴ and on alumina as well.²³

TEM. TEM pictures of a Au/TiO_2 sample that was approximately 50% reduced and one that was completely reduced are shown in Figure 9. Metallic Au particles in the range 1 to 3 nm are readily observable, but particles smaller than 1 nm could not be distinguished by this instrument. From the limited regions of the samples examined, no significant difference in the size distributions of the two samples could be observed.

CO Oxidation at 195 K. Due to the rapid reduction of Au cations in Au/TiO_2 at room temperature in a CO oxidation reaction mixture,²¹ even in the presence of excess O_2 , it is necessary to measure the catalytic activity at 195 K to avoid rapid change of the sample. At this low temperature, we have determined by XAS that the degree of reduction of a sample changed little before and after the catalytic test. Thus, it is possible to measure the CO oxidation activity for samples reduced to different degrees by H_2 pulses. In all cases, the activity declined by about 33% of its initial value with time-on-stream before reaching a pseudo-steady-state after 20 min. This pseudo-steady activity versus the degree of reduction was plotted in Figure 10. It increased roughly linearly with the degree of reduction until the catalyst was about 70% reduced (calculated from the H_2 consumption), reached a maximum at about 80% reduction, and remained constant or slightly declined upon further reduction. The activity for the fully reduced sample corresponded to $0.29 \text{ mol of CO (mol Au} \cdot \text{min)}^{-1}$.

Infrared Spectroscopy. Activation of the as-prepared catalyst by CO was studied at 213 K. The degree of reduction can be inferred from the intensity of the IR band around 2100 cm^{-1} . A band at this frequency is characteristic of CO adsorbed on metallic Au and its frequency is coverage dependent.⁶ At $213 \pm 7 \text{ K}$, the rate of reduction of Au^{3+} in the as-prepared sample was very slow under a reaction feed of CO and O_2 , and no adsorbed CO band at around 2100 cm^{-1} was observed after 65 min on stream. No reaction product was detected either. However, when a gas flow of 10% CO in He ($30 \text{ cm}^3 \text{ min}^{-1}$) was used, reduction occurred as indicated by the appearance of this IR band, as shown in Figure 11. The intensity of the IR

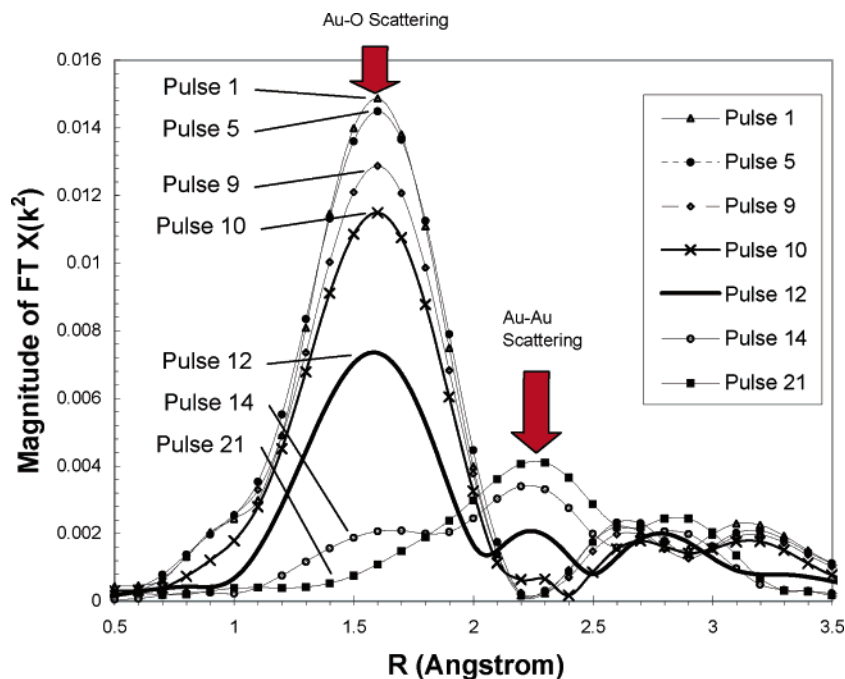


Figure 7. Magnitude of the Fourier transformed $k^2\text{-}\chi$ function in R -space of Au/TiO₂ after selected H₂ pulse. The arrows indicate positions of Au–O and Au–Au scattering at 1.6 and 2.3 Å in R -space.

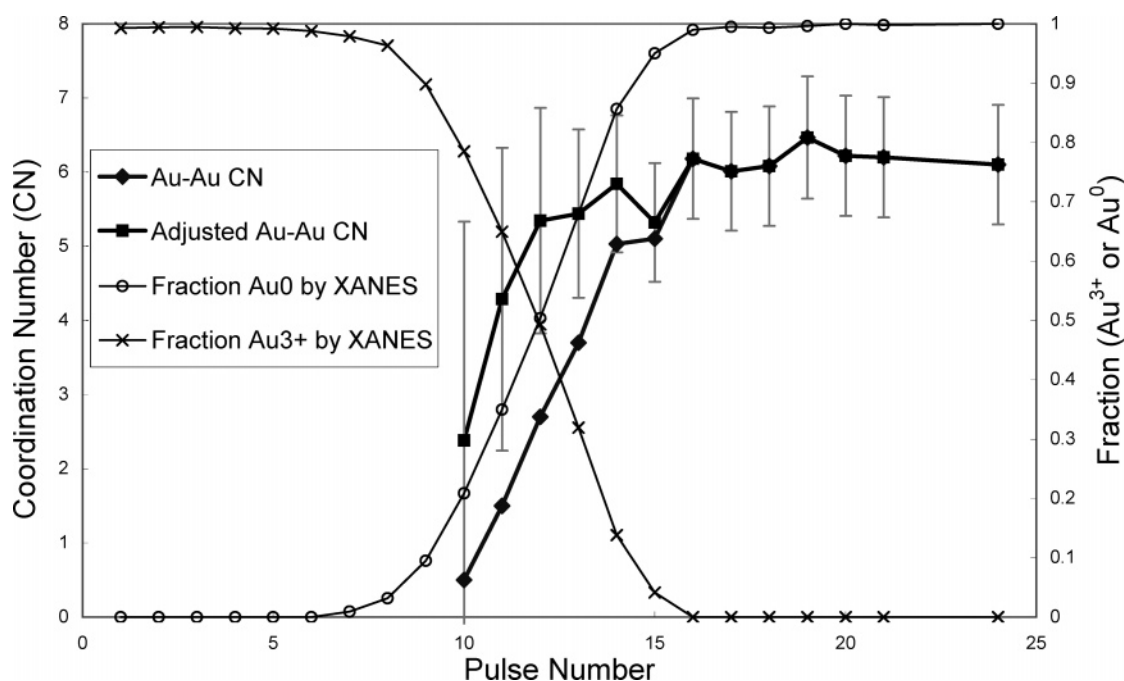


Figure 8. Au–Au coordination number obtained by fitting the $\chi(k^2)$ function (\blacklozenge), fraction of Au³⁺ (\times), and Au⁰ (\circ) obtained by XANES fit, and corrected Au–Au coordination number (\blacksquare) obtained by dividing the Au–Au CN by the fraction of Au⁰, as a function of H₂ pulse sequence.

band was very small even after 47 min on stream but subsequently increased rapidly. The band was rather broad and asymmetric, suggesting that it was a composite band.

When another as-prepared catalyst (2.8 Au wt %) was activated at 240 ± 7 K with a reaction feed of CO and O₂, oxidation activity appeared immediately, which increased together with an increase in the area of the IR band at around 2100 cm⁻¹ up to 95 min on stream, as shown in Figures 12 and 13. A group of bands between 2300 and 2400 cm⁻¹ also appeared, which were due to gas phase and adsorbed CO₂. The broad band at ~ 2100 cm⁻¹ could be deconvoluted into three peaks with peak maxima centered at 2115, 2102, and 2066 cm⁻¹.

They increased at approximately the same rate. Beyond 95 min, the CO conversion decreased slightly. At the same time, the total area of the 2100 cm⁻¹ composite band increased slightly, while the 2115 and 2102 cm⁻¹ bands remained roughly constant. In separate experiments where we activated the as-prepared sample with H₂ at room temperature and kept the sample from exposure to O₂, CO adsorption generated only bands at 2102 and 2066 cm⁻¹. The latter band intensity has a much stronger dependence on the CO pressure than the former one, as can be seen in Figure 14. Finally, the small band at 2164 cm⁻¹ did not correlate with the activation process, and its presence varied from sample to sample.

TABLE 1: Fraction of Au^{3+} and Au^0 Determined by XANES and Parameters of EXAFS Characterization^a

pulse	XANES		EXAFS					
	$\text{Au}^{3+}\text{--O}$ fraction	Au^0 fraction	scatter	CN	R , Å	DWF ($\times 10^{-3}$)	E_0	corrected Au–Au CN
0	1.0	0	Au–O	4.0	2.04	−0.9	0.7	
10	0.79	0.21	Au–O	3.8	2.04	1.0	1.0	
13	0.32	0.68	Au–Au	0.5	2.74	3.0	−6.0	2.4
			Au–O	1.6	2.04	−2.2	0.5	
16	0	1.0	Au–Au	3.7	2.74	3.0	−6.0	5.4
			Au–Au	6.2	2.75	3.4	−6.4	6.2
24	0	1.0	Au–Au	6.1	2.76	3.0	−5.9	6.1

^a First shell coordination Number (CN), bond distance (R), Debye–Waller factor (DWF), and inner potential correction (E_0). Corrected Au–Au CN obtained by dividing the Au–Au CN by the fraction of Au^0 .

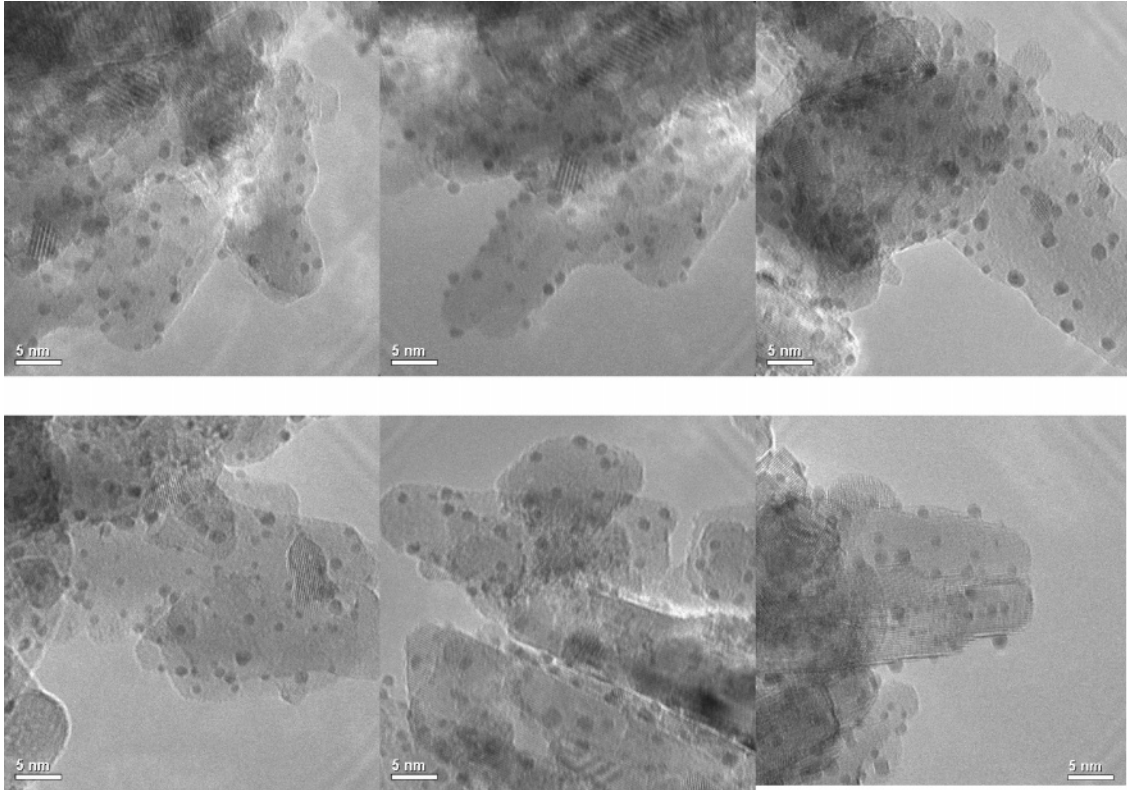


Figure 9. TEM pictures of Au/TiO_2 that were (top) approximately 50% reduced by H_2 pulses and (bottom) completely reduced by H_2 pulses.

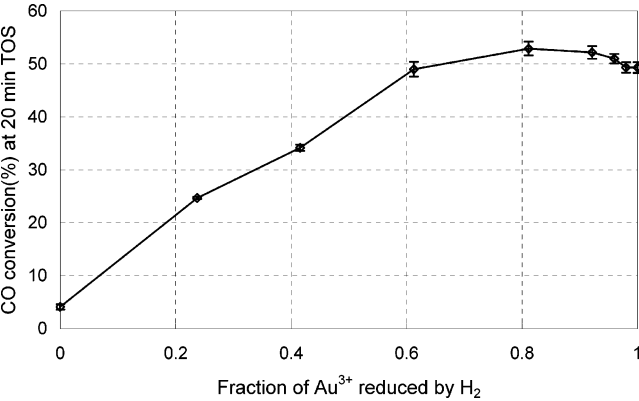


Figure 10. CO conversion of Au/TiO_2 catalyst at 20 min TOS as a function of Au^{3+} reduced by H_2 pulse. Reaction conditions: 1% CO , 2.5% O_2 , balance He , 50 mL/min, 0.1 g catalyst, 195 K.

Discussion

At the pH and Au precursor concentration used in the preparation of the catalyst here, Au exists as $\text{Au}(\text{OH})_4^-$ in solution.²³ This species and its partially dehydroxylated forms

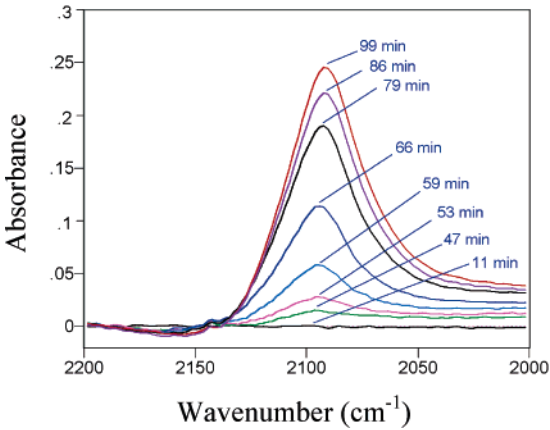


Figure 11. Infrared spectra of as-prepared Au/TiO_2 under 10% CO and balance He at 213 K.

are present in our as-prepared sample, as both H_2 consumption in the reduction experiment and XANES suggest that Au exists as Au^{3+} . Exposure of an as-prepared sample to H_2 at room temperature reduces the Au cations. Results from the H_2 pulse consumption, XAS, and microcalorimetry are all consistent with

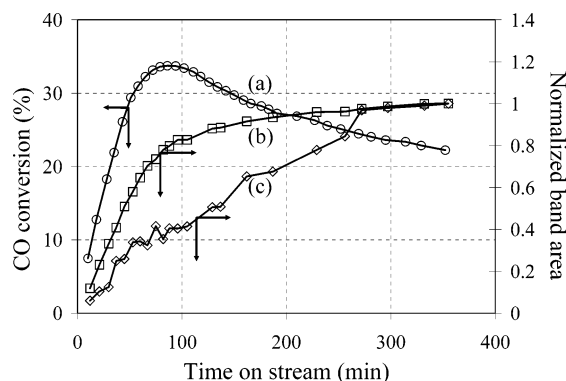


Figure 12. CO conversion (a) and the normalized intensities of the composite IR band at 2105 cm⁻¹ (b) and at 2066 cm⁻¹ (c) of an as-prepared Au/TiO₂ catalyst as a function of time-on-stream at about 240 K. Reaction conditions: 1% CO, 2.5% O₂, balance He, 11 mL/min, 10 mg of catalyst.

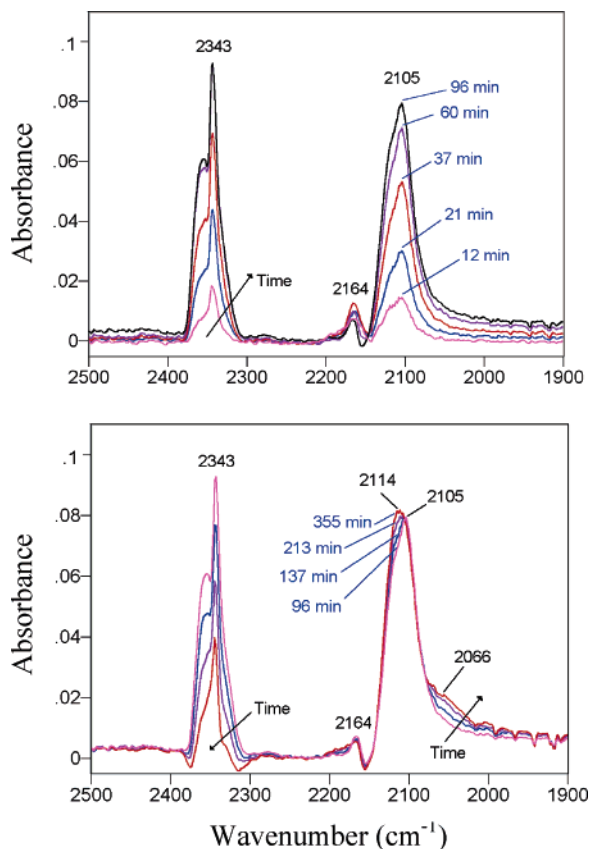


Figure 13. Time-on-stream behavior of IR spectra of Au/TiO₂ under the following reaction conditions at about 240 K: 1% CO, 2.5% O₂, balance He, 11 mL/min, 10 mg of catalyst.

the reduction process. By measuring the catalytic activity on samples reduced to different extents (Figure 10), it can be concluded that the conversion of AuO_x(OH)_{4-2x}⁻ to metallic Au is necessary for activity.

The same conclusion applies to activation by CO. The appearance of catalytic activity at about 240 K is accompanied by the formation of the 2100 cm⁻¹ composite IR band. In the presence of O₂, this composite band is composed of three bands at 2115, 2102, and 2066 cm⁻¹. If the sample is reduced by H₂, CO adsorption only generates the 2102 and 2066 cm⁻¹ bands. Thus, the 2115 cm⁻¹ band is due to CO on Au that is associated with adsorbed oxygen, consistent with the observation by Bocuzzi et al.⁶ The 2102 cm⁻¹ has been assigned to CO adsorbed on metallic Au particles.⁶ The assignment for the 2066

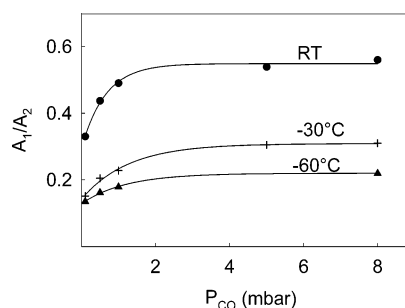


Figure 14. Ratio of the area of 2066 cm⁻¹ bands (A₁) to the area of 2102 cm⁻¹ bands (A₂) as a function of partial pressure of CO.

cm⁻¹ band is not definitive. Bocuzzi et al.²⁵ suggested that it may be the symmetric stretching mode of a Au(CO)₂ species based on the similarity of the frequency to that species isolated in a matrix.²⁶ The authors cautioned that the intense asymmetric stretching band observed in the matrix isolation study was completely absent on the supported Au catalyst. Our result, which shows that this band exhibits a stronger dependence on the CO pressure than the 2102 cm⁻¹ band, is consistent with the dicarbonyl assignment.

At near room temperature, reduction of Au³⁺ species by H₂ or CO pulses is relatively slow initially, and there is no detectable reduction in the first couple of pulses (Figures 1 and 2). In a flow containing CO, the rate of reduction is very slow at 195 K. In fact, it is slower than CO adsorption on metallic Au since a partially reduced sample can be used to catalyze CO oxidation for minutes without being further reduced by the reaction mixture. The initial reduction rate is higher at 213 K, but is still slow as an induction period is clearly observed for an as-prepared sample (Figure 11). The initial reduction rate increases with increasing temperature (Figures 12 and 13), and becomes very rapid at room temperature.²¹ Reduction by CO probably involves first associative adsorption on a Au³⁺ ion and then it is reduced either by removing an oxygen ligand as CO₂ or by reaction with a OH group to form a hydroxycarbonyl or a formate which then decomposes to CO₂. In the literature, an IR band at 2164 cm⁻¹ is assigned to CO adsorbed on cationic Au¹³ or Ti⁴⁺ ions.²⁷ This band was observed in some of our samples, but its presence could not be correlated with the extent of reduction of the sample. Associative adsorption of CO would require displacement of another ligand from the Au cation, such as water, and its rate is expected to depend on temperature and partial pressure of CO. In contrast to CO, activation of H₂ likely requires dissociative adsorption, which does not occur easily on a cation.

The induction period in the reduction of an as-prepared sample can be explained by two effects. First, adsorption and activation of the reductant (hydrogen or CO) on metallic Au are much more facile than on ionic Au. Second, Au cation species are mobile and move to metallic Au clusters where they are reduced readily by activated reductant. Thus, the initial rate of reduction is very low when the Au is ionic. The rate is substantially enhanced when the sample is partially reduced because facile activation of H₂ or CO becomes possible by the presence of metallic Au. Rapid reduction continues until eventually, the rate is limited by the availability of Au cations. It should be mentioned that instead of migration of cationic Au species, migration of metallic Au clusters or Au atoms would have the same effect.

Growth of the Au clusters is determined by the rate of formation of nucleation sites as well as the availability of AuO_x(OH)_{4-2x}⁻ species in the immediate vicinity of these

nucleation sites. Both TEM and EXAFS results indicate that the metallic Au clusters grew rapidly to 1–3 nm in size. There were very few larger particles. Although the techniques we used could not exclude the existence of much smaller Au clusters, results of a preliminary investigation using the high-resolution, Z-contrast technique in TEM that is capable of detecting isolated Au atoms, conducted by courtesy of Dr. Steven Pennycook, on selected regions of a fully reduced sample were consistent with the results reported here; that is, few isolated Au atoms or very small clusters were detected.

In the EXAFS analyses of the coordination numbers, we assumed separate phases of Au^{3+} and Au^0 . This implied that reduction of Au^{3+} did not proceed via the core–shell model: a shell of Au^0 covering a core of Au^{3+} . This is consistent with the XPS results which showed about equal quantities of Au^{3+} and Au^0 in the 50% reduced sample (Figure 4). For the core–shell model, one would expect a much higher intensity of Au^0 peaks than Au^{3+} peaks. FTIR results discussed earlier also supported this scenario. The intensity of the band for CO adsorbed on metallic Au increased with increasing extent of reduction (Figure 11).

In this study, H_2 pulse reduction was conducted using both the U-tube microreactor and the XAS sample cell. The faster reduction in the XAS cell could be due to the longer contact time of the sample with H_2 in the XAS sample cell because of back-mixing of gases and the larger pulse size. Reduction by the X-ray beam may contribute to a small extent. We observed that exposure to the beam, while not affecting an as-prepared sample initially, caused a detectable increase in the extent of reduction in a partially reduced sample. This would shorten the induction period.

In the H_2 pulse activation experiment, the activity of the Au/TiO₂ catalyst for CO oxidation at 195 K increased almost linearly with degree of reduction until about 70% reduction was reached (Figure 10). This is consistent with the picture discussed above regarding the rapid formation of small Au metal particles upon reduction. Up to 70% reduction, the major change in the sample is the increase in the number of these small metal particles, and thus the activity. Beyond 80% reduction, the increase in the number of particles is counter-balanced by increase in the particle size and changes in particle morphology, with a net result of a slight decrease in the overall activity. The latter is suggested by changes in the IR spectra. This scenario implies that not all surface metallic Au atoms are active for reaction, and we are investigating this possibility at present.

Conclusion

A more detailed picture of the activation of a Au/TiO₂ catalyst by H_2 pulse or CO reduction has emerged from this study. The process was found to begin with an induction period when sites for nucleation and hydrogen activation or CO adsorption, consisting of reduced Au species, are formed that catalyze further reduction of cationic Au species on the support. Eventually, gold particles with an average diameter of 1 to 1.5 nm are obtained. The catalytic activity for CO oxidation at 195 K increases with the extent of reduction of the sample until a maximum activity per gram of Au/TiO₂ samples is obtained at about 80% reduction, which suggests that metallic Au clusters are necessary for activity. Further reduction of the samples results in a slight decrease in catalytic activity, which was observed in both activation processes. In situ IR results suggest

that the decrease is not accompanied by a decrease in the total adsorbed CO band intensity, suggesting that it might not be due to agglomeration of Au particles but changes in the Au morphology.

Acknowledgment. The work was supported by the National Science Foundation, grant no. CTS-0121619. J.D.H. acknowledges support by the Northwestern University Institute of Environmental Catalysis funded by the Department of Energy (DE-FG02-03ER15457). The DND-CAT is supported by E.I. DuPont de Nemours & Co, Dow Chemical Co., the U.S. NSF through grant DMR-9304725, and the State of Illinois through the Department of Commerce and the Board of Higher Education Grant IBHE HECA NWU 96. The APS was supported by the U.S. Department of Energy, Office of Energy under Contract no. W-31-102-Eng-38. We gratefully acknowledge Dr. Bernd Proft of Sachtleben Chemie GmbH for providing microrutile and anatase, the Reference Catalyst Programme of the World Gold Council for providing the reference Au catalyst, and Dr. Steven Pennycook of Oak Ridge National Laboratory for collecting the Z-contrast TEM micrographs.

References and Notes

- (1) Haruta, M.; Yamada, N.; Kobayashi, T.; Iijima, S. *J. Catal.* **1989**, *115*, 301.
- (2) Bond, G. C.; Thompson, D. T. *Catal. Rev. Sci. Eng.* **1999**, *41*, 319.
- (3) Bond, G. C.; Thompson, D. T. *Gold Bull.* **2000**, *33*, 41.
- (4) Boccuzzi, F.; Chiorino, A. *J. Phys. Chem. B* **2000**, *104*, 5414.
- (5) Grunwald, J.-D.; Keener, C.; Wogerbauer, C.; Baiker, A. *J. Catal.* **1999**, *181*, 223.
- (6) Boccuzzi, F.; Chiorino, A.; Manzoli, M.; Lu, P.; Akita, T.; Ichikawa, S.; Haruta, M. *J. Catal.* **2001**, *202*, 256.
- (7) Date, M.; Ichihashi, Y.; Yamashita, T.; Chiorino, A.; Boccuzzi, F.; Haruta, M. *Catal. Today* **2002**, *72*, 89.
- (8) Wolf, A.; Schüth, F. *Appl. Catal. A: General* **2002**, *226*, 1.
- (9) Park, E. D.; Lee, J. S. *J. Catal.* **1999**, *186*, 1.
- (10) Zanella, R.; Giorgio, S.; Shin, C.-H.; Henry, C. R.; Louis, C. J. *Catal.* **2004**, *222*, 357.
- (11) Valden, M.; Lai, X.; Goodman, D. W. *Science* **1998**, *281*, 1647.
- (12) Chen, M. S.; Goodman, D. W. *Science* **2004**, *306*, 5694.
- (13) Fierro-Gonzalez, J. C.; Gates, B. C. *J. Phys. Chem B* **2004**, *108*, 16999.
- (14) Guzman, J.; Kuba, S.; Fierro-Gonzalez, J. C.; Gates, B. C. *Catal. Lett.* **2004**, *95*, 77.
- (15) Costello, C. K.; Kung, M. C.; Oh, H.-S.; Wang, Y.; Kung, H. H. *Appl. Catal. A: General* **2002**, *232*, 159.
- (16) Daté, M.; Okumura, M.; Tsubota, S.; Haruta, M. *Angew. Chem. Int. Ed.* **2004**, *43*, 2129.
- (17) Costello, C. K.; Yang, J. H.; Law, H.-Y.; Wang, Y.; Lin, J.-N.; Marks, L. D.; Kung, M. C.; Kung, H. H. *Appl. Catal. A: General* **2003**, *243*, 15.
- (18) Tsubota, S.; Cunningham, D. A. H.; Bando, Y.; Haruta, M. *Stud. Surf. Sci. Catal.* **1995**, *91*, 227.
- (19) Costello, C. K.; Guzman, J.; Yang, J. H.; Wang, Y. M.; Kung, M. C.; Gates, B. C.; Kung, H. H. *J. Phys. Chem. B* **2004**, *108*, 12529.
- (20) Schumacher, B.; Plzak, V.; Kinne, M.; Behm, R. J. *Catal. Lett.* **2003**, *89*, 109.
- (21) Kung, M. C.; Costello, C. K.; Kung, H. H. *Catalysis* **2004**, *17*, 152.
- (22) Frenkel, A. I.; Hils, C. W.; Nuzzo, R. G. *J. Phys. Chem. B* **2001**, *105*, 12689.
- (23) Yang, J. H.; Henao, J. D.; Costello, C. K.; Kung, M. C.; Kung, H. H.; Miller, J. T.; Kropf, A. J.; Regalbutto, J. R.; Bore, M. T.; Pham, H. N.; Datye, A. K.; Laeger, J. D.; Kharas, K. *Appl. Catal. A: General*. Accepted for publication.
- (24) Schwartz, V.; Mullins, D. R.; Yan, W.; Chen, B.; Dai, S.; Overbury, S. H. *J. Phys. Chem. B* **2004**, *108*, 15782.
- (25) Boccuzzi, F.; Tsubota, S.; Haruta, M. *J. Electron Spectrosc. Relat. Phenom.* **1993**, *64/65*, 241.
- (26) McIntosh, D.; Ozin, G. A. *Inorg. Chem.* **1977**, *16*, 51.
- (27) Boccuzzi, F.; Chiorino, A.; Manzoli, M. *Surf. Sci.* **2002**, *502–503*, 513.